Aeroacoustic simulation of bluff body noise using a hybrid statistical method

Con J. Doolan

School of Mechanical Engineering, The University of Adelaide, Adelaide, SA, Australia

ABSTRACT

The prediction of aerodynamic noise generated by bluff bodies is important for a broad range of technologies, such as aircraft landing gear and automotive external mirrors. However, accurate prediction is difficult and time-consuming due to the complicated flow physics that occurs in the near wake. Typically, noise predictions require computationally demanding three-dimensional flow simulations that are usually not practical for engineering use. In this paper, a method is described where two-dimensional flow simulations are used with a statistical model to introduce the effects of flow three-dimensionality into the acoustic source calculation procedure. The result is a noise prediction method that is many times faster than conventional methods. The paper will describe the method, its advantages and disadvantages and use it to simulate the noise (Aeolian tone) from a cylinder placed in a flow where its wake is turbulent (and three-dimensional). The method is shown to accurately capture the spectral broadening about the main tone.

INTRODUCTION

Aerodynamically bluff bodies are commonly used in a wide range of engineering applications and are known sources of unwanted noise when placed in a fluid stream. Examples include automotive external mirrors, aircraft landing gear, antennae on aircraft and submarines, obstructions in air ducts and a myriad of architectural design components. Given their importance to such a wide range of industries, it is important that a solid fundamental understanding of the aerodynamic bluff body noise generation mechanism is gained and secondly, that a computationally efficient means of calculating this noise is available to engineers whose task it is to design new, quiet technology in a timely manner.

The flow over a circular cylinder can be thought of as representative of most bluff body flows. Figure 1 shows a schematic representation of the wake formation process behind a circular cylinder placed in a uniform fluid stream with free stream velocity U_0. Boundary layers form on the upstream surface of the cylinder and separate when they encounter adverse pressure gradients near the top and bottom of the cylinder, forming two free shear layers. The free shear layers grow behind the cylinder, become unstable and eventually form the von Karman vortex street, a constant stream of vortices of alternate rotation that persist many diameters downstream of the cylinder. The fluid mechanics of vortex shedding behind a cylinder is a much studied topic and the review by Williamson (1996) and more recently by Rajagopalan and Antonia (2005) provide a complete background to previous work.

The oscillating velocity and pressure within the von Karman vortex street creates oscillating pressures on the surface of the cylinder. These unsteady surface pressures support dipole sources of sound, otherwise known as the Aeolian tone, first studied by Strouhal (1878). Strouhal found that the fundamental frequency (f_0) of the tone corresponds to $f_0 = St_0 U_0/D$, where $St_0 \approx 0.2$ (the fundamental Strouhal number) and D is the cylinder diameter. The spacing or spatial wavelength of the vortices (λ_v) in the wake can be related to their convection velocity $U_c = kU_0$, where $k \approx 0.6 - 0.9$, as $\lambda_v = \frac{U_c}{f_0} = D\frac{k}{St_0}$.

When the flow Reynolds number ($Re = U_0 D/\nu$, ν is the kinematic viscosity of the fluid) becomes large ($10^3 < Re$), typical of engineering applications, the wake becomes turbulent. It retains the fundamental motion of the von Karman vortex street but superimposed upon it are three-dimensional velocity fluctuations of many different wavelengths (or frequencies) and phase. This three-dimensional wake effect is also felt in the cylinder surface pressures and manifest themselves in the acoustic signature as a spectral broadening of the Aeolian tone and its harmonics. The spectral broadening is due to two effects (Norberg 2003, and references within). The first is a temporal "beating" or random amplitude modulation of the cylinder surface pressures (and sectional lift coefficient), caused by a near cylinder turbulent event (a vortex dislocation (Norberg 2003)). The second is a spanwise decorelation of surface pressure, again caused by the turbulent flow, causing each spanwise section of the cylinder to radiate noise at a different phase.

Calculation of the noise radiated from turbulent flow about a cylinder therefore requires an estimate of the effect of flow turbulence on the acoustic source terms. Theoretically, direct numerical simulation (DNS) of the Navier Stokes equations will provide all turbulence and acoustic information, but in practise, modern supercomputers will only allow direct aeroacoustic simulation for low Reynolds numbers (Inoue and Hatakeyama 2002, Müller 2008). For higher Reynolds numbers, a hybrid method is required, where a turbulent flow simulation is used with an analytical acoustic analogy (Lighthill 1952, Curle 1955) to calculate the far-field noise.

There are surprisingly few turbulent flow and noise simulations for a circular cylinder available in the literature. Seo and Moon (2007) used used Large Eddy Simulation (LES) to calculate the flow about a section of a long span cylinder. They then solved the linearised perturbed compressible equations to calculate the acoustic field. Terracol and Kopiev (2008) also used LES to simulate flow and noise about cylinders with and without a trailing edge truncation. While LES is becoming a popular methodology for modelling turbulence, it is still too computationally expensive for most engineering flows. In these cases, the unsteady Reynolds averaged Navier Stokes (URANS) equations are used. To further reduce computational overhead, two-dimensonsal simulations can also be performed.

Cox et al. (1998) performed two-dimensional URANS calculations of flow and noise for Reynolds numbers $100 \leq Re \leq 5 \times 10^6$. They found that while general agreement was obtained with experiment, the results were extremely tonal, effectively filtering out all the turbulent effects responsible for spectral broadening of the acoustic signature. Recent URANS simulations of flow and noise from cylinders with a turbulent wake (Gloerfelt et al. 2005, Cheong et al. 2008) show similar be-

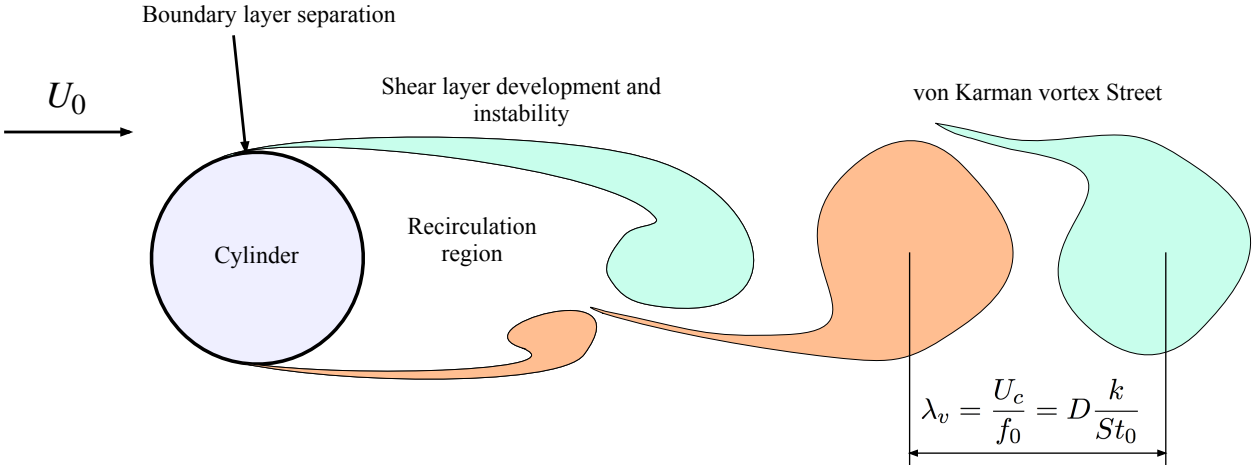

Figure 1: The development of an unsteady wake

haviour.

Casalino and Jacob (2003) developed a time-domain statistical approach of reconstructing the spanwise phase variation of surface pressures on a cylinder, originally calculated using a URANS numerical method. This method used a Ffowcs-Williams Hawkings (FWH) (Ffowcs-Williams and Hawkings 1969) method to calculate the far-field noise. Seo and Moon (2007) developed a similar methodology, however used a numerical method to calculate the far-field noise. These methods were found to work well, but still needed either ad-hoc methods (Casalino and Jacob 2003) or LES (Seo and Moon 2007) to incorporate the temporal decorrelation of individual pressure signals.

This paper will describe a method of calculating bluff body aerodynamic noise spectra using two-dimensional, URANS flow simulations to calculate the acoustic source terms. By assuming the source is acoustically compact, a simplified and more efficient acoustic analogy can be used to compute far-field sound. The method also overcomes the limitations of other approaches as it it uses a temporal decorrelation method to recreate the low-frequency beating phenomena observed in experimental lift and noise spectra. It also takes into account the spanwise variation in phase of the sectional lift coefficient by using empirically derived corellation coefficients. The method is applied to the computation of aerodynamic sound generated by turbulent flow about a circular cylinder. Aerodynamic and acoustic results are compared with experimental data from the literature.

AERODYNAMIC SIMULATION METHOD

Computational Details

Flow simulations were performed using the open source numerical simulation code OpenFOAM (Weller et al. 1998) to solve the Unsteady Reynolds Averaged Navier Stokes (URANS) and continuity equations (see Leclercq and Doolan (2009) for numerical implementation). Turbulence closure was provided by the realisable k-epsilon model (Shih et al. 1995).

The equations were discretised using a structured finite-volume method within the openFOAM software package. The convective and diffusive terms were evaluated using a second-order accurate upwind method. Time integration was performed using a second order implicit backward differencing method with the requirement that the maximum Courant number was kept below 0.2. The pressure-implicit split-operator (PISO) algorithm with two correction steps was used as an implicit, transient solution scheme. The resulting system of equations were solved using the incomplete Choleski conjugate gradient method with a solution tolerance of 10^{-6}.

Test Case: Single Cylinder

The test case is the simulation of flow and noise from a cylinder at a Reynolds number $Re = U_0 d/\nu = 22,000$ (ν = kinematic viscosity). The particular simulation is identical to the aeroacoustic experiments presented in Casalino and Jacob (2003). They are also very close to the experiments of Schewe (1983) who measure the unsteady forces developed on a cylinder at $Re = 23,000$. A combination of results from Casalino and Jacob (2003) and Schewe (1983) will be used for comparison purposes.

The flow calculations were carried out on a mesh that contained 45,234 orthogonal cells arranged in a C type mesh about the cylinder (see Fig. 2). The mesh was constructed so that the outer boundaries were all $16d$ from the cylinder centre. No-slip boundary conditions were applied to the cylinder surface while standard inlet and outlet boundary conditions were applied to the outermost cells. The cell height used at the cylinder surface was $0.0075d$. This resolution was found to be adequate to resolve the boundary layer and achieve an accurate aerodynamic simulation when compared with experiment. As the flow about the cylinder is *sub-critical* (Norberg 2003, for definition of critical states), laminar boundary layers occur on the cylinder surface, followed by transition in the separated shear layer. It was found that the realisable k-epsilon model (Shih et al. 1995) was able to mimic this behaviour and simulate the aerodynamic forces correctly at this Reynolds number.

To simulate the freestream turbulence intensity of the comparison experiments ($I = 0.41\%$) (Casalino and Jacob 2003), the non-dimensionalised turbulent inlet boundary conditions were assumed to be $k/U_0^2 = 3/2I^2 = 2.5\times10^{-5}$ and $\varepsilon d/U_0^3 = C_\mu Re(k^2/U_0^4)(\nu_t/\nu)^{-1} = 1.2375\times10^{-6}$ with $C_\mu = 0.09$ (Launder and Sharma 1974) and the ratio of freestream turbulent eddy viscosity to molecular viscosity $(\nu_t/\nu) \approx 1$.

The single cylinder simulations were carried out using a non-dimensional time step of $\Delta t U_0/d = 0.001$. Simulations were impulsively started by setting all cells with velocity $[U_1/U_0, U_2/U_0]^T = [1,0]^T$ and relative pressure $P = 0$. It takes approximately 15,000 time steps or a non-dimensional time of 15 for vortex shedding to begin. All initial flow transients disappeared by $tU_\infty/D = 175$ or 5.4 computational domain flow-through times. Flow simulations were obtained after the initialisation period for $tU_\infty/D = 434.783$ non-dimensional time units or 13.59 domain

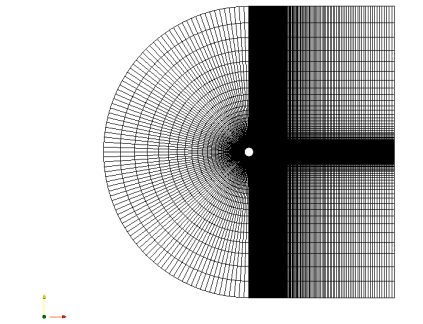

(a) Entire grid

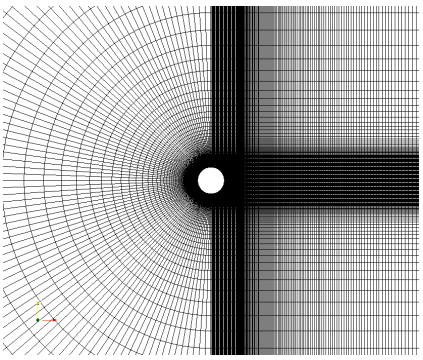

(b) Region about cylinder

Figure 2: Computational grid used for aerodynamic simulation

flow-through times. This corresponds to 434,783 time steps and captures 100 vortex shedding cycles with 439 non-dimensional time steps per shedding period.

ACOUSTIC SIMULATION METHOD

Compact Acoustic Assumption

It is pertinent to examine the limits of acoustic compactness before describing the general acoustic simulation methodology. An assumption of acoustic compactness is valid if the wavelength of sound is greater than the dimensions of the object or source region producing it. Strictly, it is difficult to determine definite frequency limits on when compactness can be assured. This is because as the wavelength to source dimension ratio (λ/d) is increased, true compactness is achieved only asymptotically as $\lambda/d \to \infty$. Practically however, a nearly compact sound field is achieved before that and, as will be shown below, the error in this assumption is limited to a ~ 1 dB if the Mach number is small.

Consider a cylinder of diameter d in cross flow whose freestream velocity is U_0 and Mach number M. The sound above the cylinder is mainly controlled by the dipole sound field whose source strength is governed by the surface pressure fluctuations. If the sound is measured directly above the cylinder, a distance R from its centre, then Curle's theory can be used to approximate its value ($p'(\omega)$)

$$p'(\omega) \sim \frac{-i\omega A}{(c_0 R)} \left(p_u e^{\frac{-i\omega(R-d/2)}{c}} - p_l e^{\frac{-i\omega(R+d/2)}{c}} e^{-i\xi} \right) \quad (1)$$

$$\sim \frac{-i\omega A}{(c_0 R)} |p| e^{-i\omega R/c} \left(e^{\frac{i\omega d}{2}} - e^{\frac{-i\omega d}{2}} e^{-i\xi} \right) \quad (2)$$

where p_u and p_l are the pressures on the upper and lower surface of the cylinder, $|p| \sim |p_u| \sim |p_l|$, A is a reference area and ξ is the phase between p_u and p_l. If a compact assumption is made, then the propagation time between points on the surface is zero, or in the above equation $d \to 0$. Therefore, an estimate of the error due to a compact assumption can be made by dividing Eq. 2 by itself but with $d = 0$. In dB, this expression is (taking the real component)

$$\mathscr{E} = 20 \log_{10} \cos(\pi St M) \quad (3)$$

For the case considered here, the maximum frequency is limited to a Strouhal number, $St = fd/U_0 = 2$ and a Mach number of 0.06. This results in an error $\mathscr{E} < 1$ dB. Therefore the assumption of compactness is appropriate for the present work. Note that the error becomes very large when $M > 0.15$.

Curle's Theory

The acoustically compact form of Curle's equation (Curle 1955) can be simplified to predict the acoustic far field (represented as a density fluctuation ρ') generated at an observation point by a fluctuating point force $\bar{F}$ applied on a compressible fluid that is initially at rest

$$4\pi c_0^2 \rho'(\tilde{x},t) = -\frac{\partial}{\partial x_i}\left[\frac{F_i}{r}\right] = \frac{1}{c_0}\frac{x_i}{r^2}\left[\frac{\partial F_i}{\partial t}\right] \quad (4)$$

where F_i are the three vector components of the resulting force applied on the fluid and c_0 is the speed of sound of the medium (air) at rest. The observation point is $\tilde{x}$ measured with respect to the compact body (in this case, the centre of the cylinder). The distance between the body and the observation point is described by the distance r. The square brackets denote a value taken at the retarded time $\Theta = t - r/c_0$.

A URANS simulation can provide unsteady sectional force data ($F_i(t)$, used to calculate the acoustic source terms in Curle's compact acoustic analogy, Eq. 4) in a straightforward manner. However, it is well known that transient force data from these types of simulations are extremely tonal and tend to overestimate the vortex shedding frequency, and its harmonics, resulting in poor noise predictions. The reasons behind these deficiencies results from the two-dimensionality of the simulation and, to some extent, the nature of the turbulence model employed (Casalino et al. 2003). The frequency change is mainly due to the over-prediction of Reynolds stresses in the near wake artificially constraining the size of the re-circulation bubble formed immediately behind the bluff body (Roshko 1993).

To use a URANS simulation to calculate noise, the simulated body forces need to be modified to take into account the effect of wake three-dimensionality on the cylinder unsteady sectional force coefficients. This is done in a two-step method. First, the random, low frequency beating is introduced using a temporal model. Second, the effects of spanwise decorrelation are incorporated using a modified form of the model originally developed by Casalino and Jacob (2003). These models are summarised below.

Temporal Model

It is assumed that the true force $F_{true}(t)$ is convoluted over a signal of time length T to the URANS simulated force signal $F_{URANS}(t)$ using an impulse response function $h(t)$

$$F_{true}(t) = \int_0^T h(\tau) F_{URANS}(t)\, d\tau \quad (5)$$

If the impulse response function can be described as

$$h(t) = e^{-i\phi_\tau} \quad (6)$$

then the true signal can be considered as a composite of a number of original simulated signals, each with a randomly dispersed phase difference $\phi_\tau = \phi_\tau(\tau)$.

In the same manner as the spatial case (Casalino and Jacob 2003, see next section), it is assumed that the autocorrelation coefficient (ρ_τ) can be distributed according to Laplacian statistics

$$\rho_\tau(\tau) = \exp\left(-\frac{\tau_t}{\tau_c}\right) \tag{7}$$

so that $\tau_t = \tau/T$ is the time delay normalised by the time base T and $\tau_c = \Delta t_c/T$ is a normalised time scale associated with the randomness of the time signal. Note, Gaussian statistics could equally be applied.

The Laplacian model calls for a linear distribution of variance over $0 \leq \tau_t \leq 1$

$$w_\tau(\tau_t) = w_{\tau,max}\tau_t \tag{8}$$

where $w_{\tau,max} = 1/\tau_c$. This variance distribution is used to generate a random dispersion of phase (ϕ_τ) over $0 \leq \tau_t \leq 1$ that modulates the retarded time of the URANS signal used to calculate noise in Eq. 4 using

$$\Theta_\tau = \Theta + \frac{\phi_\tau}{2\pi}\frac{d}{U_0} \tag{9}$$

This modulation is performed as a pre-processing step before the spanwise decorrelation of the signals. Practically, 100 URANS unsteady force data records, each with a randomly dispersed phase, are used to create a single temporally decorrelated force signal.

Spatial Model

Recently, Casalino and Jacob (2003) have developed an ad-hoc technique to overcome some of the problems associated with URANS solutions in noise prediction. It accounts for the three-dimensional nature of the flow by randomly dispersing the phase of surface pressure fluctuations across the span of a cylinder (or any other extruded two-dimensional shape) according to a statistical model based on an estimate of the spanwise coherence. The random phase is then used to perturb the retarded time of surface pressure fluctuations across the span, which are then used in an FWH solver to calculate far-field noise.

Following Casalino and Jacob (2003) and consistent with the temporal model of the last section, random phase distributions are determined using a linear variance distribution (w) across the span

$$w(\eta) = 2w_{max}|\eta| \tag{10}$$

where η is the the spanwise coordinate along the cylinder span (L_z). A linear variance distribution results in a Laplacian correlation coefficient, giving

$$w_{max} = 1/L_l \tag{11}$$

where L_l is Laplacian spanwise correlation length scale. Hence, the model describing the correlation coefficient $\rho(\eta)$ across the span is (for Laplacian statistics)

$$\rho(\eta) = \exp\left(-\frac{|\eta|}{L_l}\right) \tag{12}$$

Using the spanwise statistical model, a random dispersion in phase (ϕ_η) is created along the span of the cylinder.

The phase distribution is then used to modulate the retarded time

$$\Theta_\eta = \Theta + \frac{\phi_\eta}{2\pi}\frac{d}{U_0} \tag{13}$$

This procedure is equivalent to introducing a spanwise loss of coherency along the span of a cylinder. It is a convenient way of introducing some of the features of a three-dimensional flowfield to a noise calculation that uses a two-dimensional flow simulation.

To estimate the spanwise correlation length scale, empirical relations (Norberg 2003) can be used. For this paper, the experimental measurements of Casalino and Jacob (2003) are used instead.

Frequency Compensation

The experimental data has been shifted in frequency so that the main tone occurs at an identical Strouhal number to the URANS simulation. According to Curle's theory (Eq. 4), linear frequency scaling also necessitates a small scaling in amplitude. The frequency and amplitude were scaled according to

$$f_{shift} = f\frac{St_{\text{num}}}{St_{\text{exp}}} \tag{14}$$

$$\Delta\text{SPL(dB)} = 20\log_{10}\frac{St_{\text{num}}}{St_{\text{exp}}} \tag{15}$$

RESULTS

Aerodynamic Results

Figure 3 shows the instantaneous spanwise vorticity in the near wake of the cylinder over one vortex shedding cycle. The simulation successfully recreates the major features of the unsteady flow. These are boundary layer separation, shear layer growth and instability and the creation of discrete vorticies that later form the von Karman vortex street. While the URANS modelling procedure filters most of the high frequency turbulence fluctuations, small vorticial structures form in the shear layers and these may be attributed to the Kelvin-Helmholtz instability mechanism. The periodic nature of the shedding process observed in Fig. 3 is responsible for the creation of unsteady force on the cylinder and hence noise.

Table 1 compares mean flow measurements from the literature with the numerical simulations. As shown, the URANS simulation recreate the mean force coefficients well. The fundamental Strouhal number (St_o) is slightly over-predicted and the reasons for this are discussed earlier.

Equispaced contours of root-mean-square (RMS) pressure coefficient about the cylinder are shown in Fig. 4. The highest level of pressure fluctuation is present in the flow itself, in the region of the near wake associated with vortex formation. However, this pressure variation does not contribute significantly to the farfield noise. This is because it is not near a solid boundary and hence cannot support a dipole (Curle 1955). In fact, the acoustic

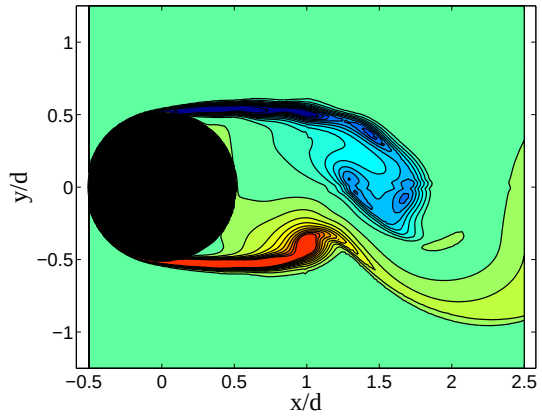

(a) $tU_0/D = 321$

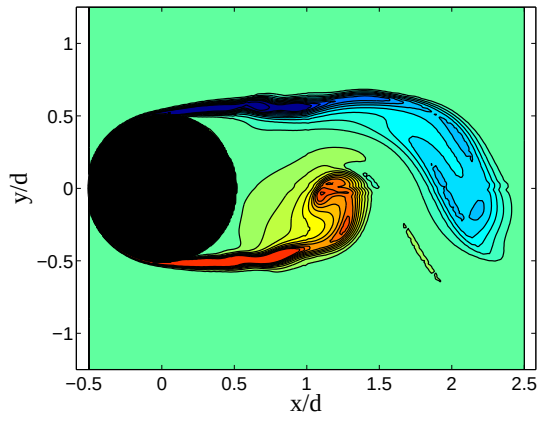

(b) $tU_0/D = 322$

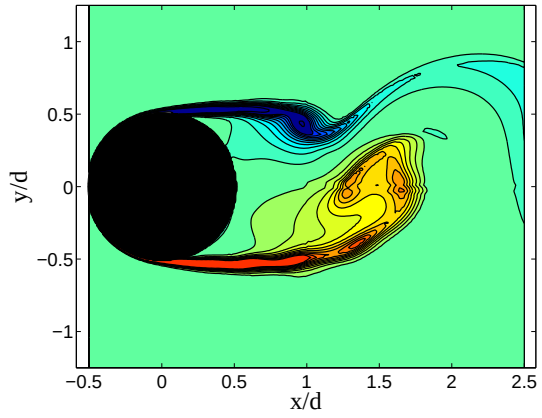

(c) $tU_0/D = 323$

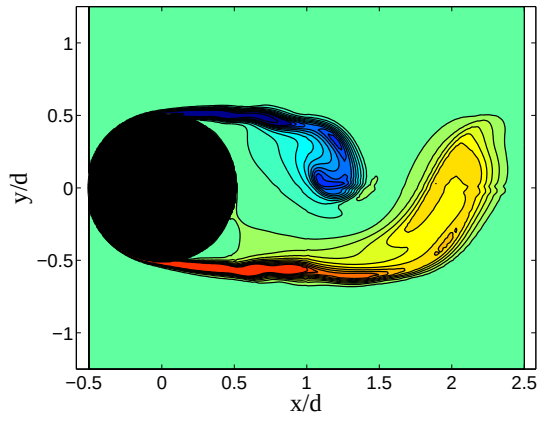

(d) $tU_0/D = 324$

Figure 3: Instantaneous spanwise vorticity contours over one vortex shedding cycle. Levels: $-15 \leq \frac{\omega_z d}{U_\infty} \leq 15$ with intervals $\frac{|\Delta\omega|d}{U_\infty} = 5$

Table 1: Comparison between mean experimental data and URANS simulation data.

	Experiment	URANS
St_0	0.2*	0.239
C_l'	0.354**	0.367
$\overline{C}_d$	1.1**	0.98

Source: *(Casalino and Jacob 2003),**(Schewe 1983)

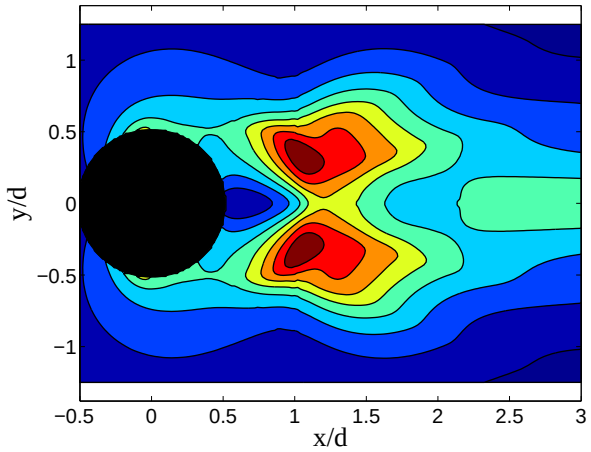

Figure 4: RMS pressure coefficient contours about the cylinder in turbulent flow. Levels: $0 \leq p_{rms}/(\rho_0 U_0^2) \leq 0.225$ with intervals $\Delta p_{rms}/(\rho_0 U_0^2) = 0.025$

source associated with the wake is of quadrupole form and is therefore very inefficient compared with pressure variations on the surface of the cylinder (Lighthill 1952).

For this case, the unsteady pressure that is the major contributor to noise is that on the surface of the cylinder. From Fig. 4, the largest unsteady pressure amplitudes occur on the top and bottom surfaces of the cylinder, hence it is the lift dipole that is the largest source of noise. This is consistent with the conventional model for the production of the Aeolian tone (Phillips 1956). However, the unsteady drag, while lower in amplitude, can still provide a significant component to the measured noise spectra if the measurement microphone is placed away from the vertical axis (Casalino and Jacob 2003, Lockard et al. 2008)

Time-series unsteady sectional lift and drag coefficient data obtained from the URANS aerodynamic simulation are presented in Fig. 5 over a non-dimensional time of $\Delta t U_0/D = 100$. The force signals are periodic and statistically stationary. It is interesting to observe that the drag force oscillates at twice the frequency of the lift force. This is due to the fact that the sign of the resolved vertical (lift) forces depends on the sign of the shed vorticity, but the resolved horizontal (drag) forces are independent of the sign of the vorticity.

Figure 6 displays the power spectra of the simulated force coefficients. The spectra are extremely tonal, with significant harmonic components. If these are used to calculate noise, they will give unrealistically tonal noise spectra. The acoustic simulation method described earlier will be used in the next section to obtain acoustic spectra that contain the correct amount of spectral broadening.

Acoustic Results

Before effective acoustic simulation can be performed, estimates of the time and space correlation scales are required for the statistical analysis.

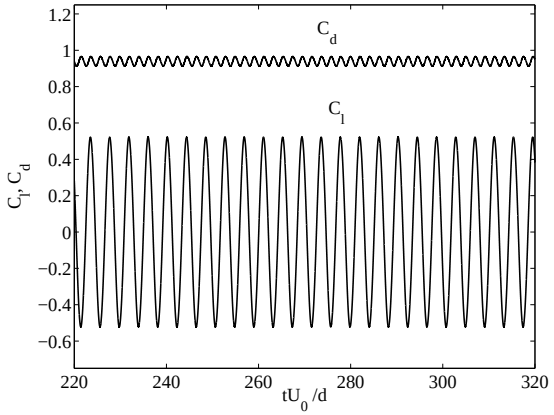

Figure 5: Unsteady lift and drag coefficients

Estimation of the time scale used for temporal decorrelation of the sectional force coefficients (i.e. τ_c) is difficult. Some guidance can be found in examining experimental unsteady surface pressures records Norberg (2003). It is assumed here that disturbances can be expected to occur at about every $N_\tau = 60$ vortex shedding periods. Assuming this is approximately equal to the maximum standard deviation of the time-shift used to decorrelate the signals, $\tau_c \sim \left(\frac{2\pi N_\tau}{St_0}\right)^{-2} \sim 10^{-6}$. This is a crude estimate of the time scale however, as shown below, it produces reasonable results.

Casalino and Jacob (2003) obtained spanwise surface pressure correlation measurements on a cylinder in cross flow at a Reynolds number of $Re = 22,000$, and these are used for the present study. A statistical model was fitted to these data for various correlation length scales (L_l). For the present study, a spanwise correlation length scale of $L_l/L_z = 0.27$ will be used to estimate far-field noise spectra (L_z is the cylinder span, taken to be 0.3 m to match the experiments).

The computed acoustic data will be compared against the experimental data of Casalino and Jacob (2003). The particular experimental case was performed at identical aerodynamic conditions as the simulation and at a microphone location directly above the cylinder, at a non-dimensional distance of $r/D = 86.25$ from the cylinder centre. The spectral resolution of the experiments was reported to be 2 Hz (or $\Delta St = 0.0016$).

Figure 7(a) shows the computed time-series acoustic pressure at the identical location as the experiment. The statistical method has the effect of introducing amplitude modulation into the signal. The method shows a random, beating of the signal, similar to experiment (Norberg 2003).

Figure 7(b) shows the spectral density of the computed acoustic signal, compared with experiment. Figure 7(b) was computed by averaging 100 spectra, each generated from a different random seed (labelled URANS + Statistics). The spectral resolution of these results is 2.98 Hz ($\Delta St = 0.0024$). Also shown in Fig. 7(b) is the computed spectra using the unmodified URANS unsteady force coefficient data as input (labelled URANS).

The comparison between computation (URANS + statistics) and experiment is good. The method is able to provide a reasonable amount of spectral broadening and recreates the broadband levels at higher Strouhal numbers (frequency, $f = StD/U_0$). The method was not successful in recreating the spectral broadening about the first lift harmonic. The reasons for this are not yet clear. It is probable that more refined estimates of τ_c are required. As expected, the comparison between the spectra calculated using the unmodified URANS unsteady force data and experiment is poor.

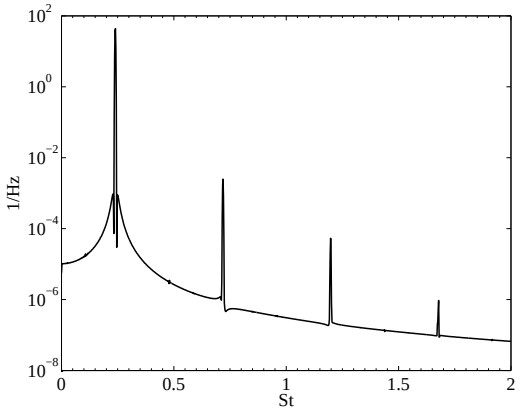

(a) Lift coefficient spectrum

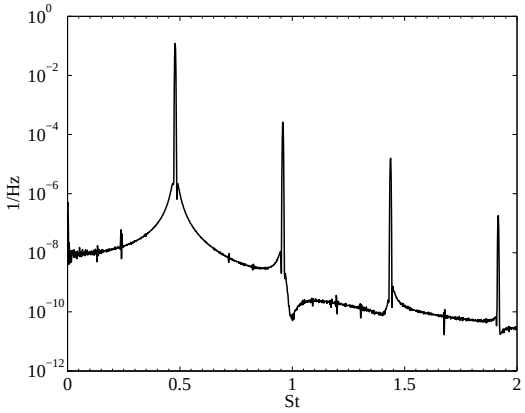

(b) Drag coefficient spectrum

Figure 6: Lift and drag coefficient power spectra.

CONCLUSION

A hybrid method for calculating aerodynamic bluff body noise spectra using two-dimensional URANS unsteady force data to construct the source terms is presented. To take into account three-dimensional wake flow effects on the computed noise, a statistical method that decorrelates the tonal URANS signals is developed.

The method is applied to the case of Aeolian tone generation from a cylinder in a cross flow with a turbulent wake. Assuming that the cylinder is acoustically compact is justified and simplifies the application of an acoustic analogy to calculate far-field sound. Aerodynamic simulation results show that the major features of flow field are recreated, apart from key information regarding the spectral content of the sectional force coefficients. This information is recreated using the statistical model. When applied to the experimental test case, a good comparison is obtained.

REFERENCES

J Ask and L Davidson. The sub-critical flow past a generic side mirror and its impact on sound generation and propagation. *Proceedings of the 12th AIAA/CEAS Conference, MA, USA*, 2006.

D. Casalino and M. Jacob. Prediction of aerodynamic noise from circular rods via spanwise statistical modelling. *Journal of Sound and Vibration*, 262:815–844, 2003.

D. Casalino, M. Jacob, and M. Roger. Prediction of rod-airfoil interaction noise using the fw-h analogy. *AIAA Journal*, 41 (2):182–191, Feb 2003.

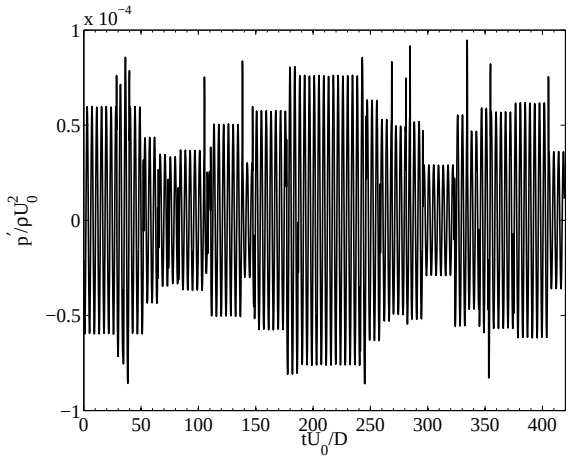

(a) Time series acoustic pressure

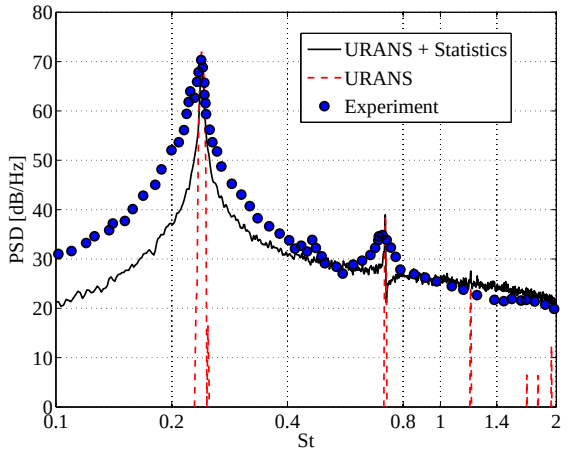

(b) Acoustic power spectrum

Figure 7: Acoustic pressure, compared with experiment

C Cheong, P Joseph, Y Park, and S Lee. Computation of aeolian tone from a circular cylinder using source models. *Applied Acoustics*, 69(2):110–126, Feb 2008. doi: 10.1016/j.apacoust.2006.10.004.

JS Cox, KS Brentner, and CL Rumsey. Computation of vortex shedding and radiated sound for a circular cylinder: subcritical to transcritical reynolds numbers. *Theor Comp Fluid Dyn*, 12(4):233–253, 1998.

N. Curle. The influence of solid boundaries on aerodynamic sound. *Proc. Roy. Soc. London*, A231:505–514, 1955.

J Ffowcs-Williams and D Hawkings. Sound generation by turbulence and surfaces in arbitrary motion. *Proc. Roy. Soc. London*, A264(1151):321–342, Jan 1969. URL `http://journals.royalsociety.org/index/U4M23M5356406553.pdf`.

X Gloerfelt, F Pérot, C Bailly, and D Juvé. Flow-induced cylinder noise formulated as a diffraction problem for low mach numbers. *Journal of Sound and Vibration*, 287:129–151, Jan 2005.

O. Inoue and N. Hatakeyama. Sound generation by a two-dimensional circular cylinder in a uniform flow. *J. Fluid Mech.*, 471:285–314, Jan 2002.

B.E. Launder and B.I. Sharma. Application of the energy dissipation model of turbulence to the calculation of flow near a spinning disc. *Letters in Heat and Mass Transfer*, 1(2):131–138, April 1974.

D.J.J. Leclercq and C.J. Doolan. The interaction of a bluff body with a vortex wake. *Journal of Fluids and Structures (Accepted 7/3/09)*, 25(5), 2009.

M.J. Lighthill. On sound generated aerodynamically: General theory. *Proc. Roy. Soc. London*, A221:564–587, 1952.

David P Lockard, Meelan M Choudhari, Mehdi R Khorrami, Dan H Neuhart, Florence V Hutcheson, Thomas F Brooks, and Daniel J Stead. Aeroacoustic simulations of tandem cylinders with subcritical spacing. In *Paper No. AIAA-2008-2862*, 14th AIAA/CEAS Aeroacoustics Conference, 2008.

B Müller. High order numerical simulation of aeolian tones. *Computers and Fluids*, 37(4):450–462, 2008.

C. Norberg. Fluctuating lift on a circular cylinder: review and new measurements. *Journal of Fluids and Structures*, 17:57–96, 2003.

OM Phillips. The intensity of Aeolian tones. *Journal of Fluid Mechanics*, 1, 1956.

S Rajagopalan and R Antonia. Flow around a circular cylinder—structure of the near wake shear layer. *Experiments in Fluids*, 38:393–402, 2005. URL `http://www.springerlink.com/index/NLH5BJD737TFYLV2.pdf`.

James D Revell, Roland A Prydz, t, and Anthony P Hays. Experimental study of aerodynamic noise vs drag relationships for circular cylinders. *AIAA Journal*, 16(9):889–897, Aug 1978.

A. Roshko. Perspectives on bluff body aerodynamics. *Journal of Wind Engineering and Industrial Aerodynamics*, 49:79–100, 1993.

G. Schewe. On the force fluctuations acting on a circular cylinder in crossflow from subcritical up to transcritical reynolds numbers. *Journal of Fluid Mechanics*, 133:265–285, 1983.

J Seo and Y Moon. Aerodynamic noise prediction for long-span bodies. *Journal of Sound and Vibration*, 306:564–579, Jan 2007. URL `http://linkinghub.elsevier.com/retrieve/pii/S0022460X07004130`.

TH Shih, WW Liou, A. Shabbir, and J. Zhu. A new ke eddy-viscosity model for high reynolds number turbulent flows-model development and validation. *Computers Fluids*, 24(3):227–238, 1995.

V. Strouhal. Ueber eine besondere Art der Tonerregung. *Annalen der Physik und Chemie*, 241(10), 1878.

M Terracol and V Kopiev. Numerical investigation of the turbulent flow around a truncated cylinder: noise reduction aspects. *14th AIAA/CEAS Aeroacoustics Conference (29th AIAA Aeroacoustics Conference)5 - 7 May 2008, Vancouver, British Columbia Canada*, AIAA 2008-2868:11, May 2008.

H.G. Weller, G. Tabor, H. Jasak, and C. Fureby. A tensorial approach to cfd using object orientated techniques. *Computers in Physics*, 12(6):620–631, 1998.

CHK Williamson. Vortex dynamics in the cylinder wake. *Annual Review of Fluid Mechanics*, 28(1):477–539, 1996.